SIBi

SISTEMA INTEGRADO DE BIBLIOTECAS
UNIVERSIDADE DE SÃO PAULO

Universidade de São Paulo

Biblioteca Digital da Produção Intelectual - BDPI

Departamento de Metalúrgica e de Materiais - EP/PMT

Artigos e Materiais de Revistas Científicas - EP/PMT

2013-02

Effect of Prior Photodegradation on the Biodegradation of Polypropylene/Poly(3-hydroxybutyrate) Blends

Effect of Prior Photodegradation on the Biodegradation of Polypropylene/Poly(3-hydroxybutyrate) Blends

Roberta K. Sadi,[1] Guilhermino J.M. Fechine,[2] Nicole R. Demarquette[1]

[1] Metallurgical and Materials Engineering Department, University of São Paulo, Avenida Professor Mello Moraes, 2463 São Paulo, Brazil

[2] Materials Engineering Department, Mackenzie Presbyterian University, Rua da Consolação, 930 São Paulo, Brazil

In this work, the effect of blend composition and previous photodegradation on the biodegradation of polypropylene/poly(3-hydroxybutyrate) (PP/PHB) blends was studied. The individual polymers and blends with or without the addition of poly(ethylene-*co*-methyl acrylate-*co*-glycidyl methacrylate) [P(E-MA-GMA)] as a compatibilizer (in the case of 80/20 blend) were exposed to UV light for 4 weeks and their biodegradation was evaluated. The biodegradation of PHB phase within the blends was hindered as PHB was the dispersed phase and PP fibrous particles were observed at the surface of the blend samples after biodegradation. Previous photodegradation lessened PHB biodegradation but enhanced the biodegradation of PP and the blends within the biodegradation time studied. Photodegradation resulted in cracks at the surface of PP and the blends, which probably facilitated the biotic reactions due to an easier access of the enzymes to deeper polymer layers. It also resulted in a decrease of molecular weight of PP phase and formation of carbonyl and hydroxyl groups which were consumed during biodegradation. Size exclusion chromatography analysis revealed that only the short chains of PP were consumed during biodegradation. POLYM. ENG. SCI., 53:2109–2122, 2013. © 2013 Society of Plastics Engineers

INTRODUCTION

The search for sustainable development has led for the last two decades to a growing interest in the development of biodegradable polymers. They can originate from biomass such as cellulose and starch, from microbial production such as polyhydroxyalkanoates, from chemical synthesis using monomers from agro-resources such as poly(lactic acids), or monomers from fossil resources such as polycaprolactones, for example [1–3]. These polymers can normally be degraded by the action of micro-organisms such as bacteria and fungi within a reasonable amount of time [3] that can vary according to the different authors from a few months to 2 years.

Poly(hydroxyalkanoates) (PHA) are natural biodegradable polyesters that are synthesized as storage materials by several micro-organisms in the presence of a carbon source such as sugar or oil [4]. Poly(3-hydroxybutyrate) (PHB in the remaining of the text),one of the main PHAs, is a very fragile polymer due a high crystallinity varying from 50 to 80% and large spherulitic structures. It is also unstable with time [4, 5, 6] and presents a difficult processing: its processing window is rather small as the melting temperature or is very close to its degradation temperature [7].

In order to cope with these limitations, it is possible to blend PHB with other polymers and many efforts have been spent to optimize the properties of blends containing PHB either as a matrix or dispersed phase [2, 8]. In this work, PHB was added to polypropylene (PP) in an attempt to obtain a blend with reasonable mechanical properties while conferring some biodegradability to the material. In a previous article, we reported that it was possible through a suitable compatibilization to obtain PP/PHB blends with good mechanical properties [9]. However, as micro-organisms do not manage to metabolize PP within an acceptable frame of time, even when it is mixed with PHB, one should not expect the blend to be biodegradable.

It has been reported in the literature that prior photodegradation could be a nice tool to enhance biodegradation of non-biodegradable or even biodegradable polymers. Prior photodegradation has been shown to enhance biodegradation of polyolefins [14–17] in this case, photodegradation normally results in oxygenated chemical bounds and shorter chains which are normally more easily consumed by micro-organisms, turning the polymer more accessible for microbial assimilation. In the case of biodegradable

polymer [14–17], the effect of prior degradation depends on the chemical nature of the polymer and the stage of biodegradation, prior photodegradation may delay biodegradation in the first stages of the biotic process due to a crystallinity increase induced by photodegradation at the surface (in the case of PHB, for example) [17] and may increase biodegradation in the following stages due to the chain scissions also undergone during UV exposure. In the case of blends and composites, very few studies have been published on the effect of prior photodegradation on biodegradation. To the authors knowledge, it has been studied only in the case of polyolefins/starch blends [low-density polyethylene (LDPE)] [18–20] or PP [21] and polyolefins/cellulose composites (PP [22, 23] or LDPE [24]), but the results are still controversial. In some cases, photodegradation was shown to enhance biodegradation [19] due to the oxidation of the polyolefin while in others it was shown not having a large effect on biodegradation due to crosslinking reactions that were created between the polyolefins and the cellulose during the photodegradation step [22, 24]. The small amount of studies on the effect of prior photodegradation on biodegradation of blends is probably due to the fact that the mechanisms governing photodegradation of blends and composites are still not very well understood [25, 26] due to their complexity. The study of the effect of prior photodegradation on biodegradation is, however, of prime importance as polymers which will be littered could be exposed to solar radiation, and, as a consequence, be subjected to the combined effect of UV light and biological factors, therefore, more work should be conducted on the subject.

It is well known that the properties of immiscible polymer blends depend on their morphologies, which can be controlled during processing, through a proper choice of the rheological properties of the polymers and efficient compatibilization [27, 28]. Biodegradability is not an exception [20, 29–37]. If a biodegradable polymer is added to a nonbiodegradable polymer, the biodegradability of the resultant material will also depend on its morphology. If the nonbiodegradable polymer is the dispersed phase, its presence will result in an enhanced decomposition of the biodegradable polymer, as the surface area for biotic reaction of the matrix will increase [17, 36]. If the nonbiodegradable polymer is the matrix phase, a certain concentration of biodegradable polymer will need to be added for the material to be considerably degraded by the micro-organisms. Wool et al. [31, 32] using both experimental data and mathematical simulations showed that biodegradation of polyethylene (PE)/starch blends depends on the thickness of the sample, dispersed phase particle diameter, concentration of dispersed phase, percolation threshold, and microbial population. When the starch fraction is higher than the percolation concentration, pathways for micro-organisms are created and biodegradation is accelerated.

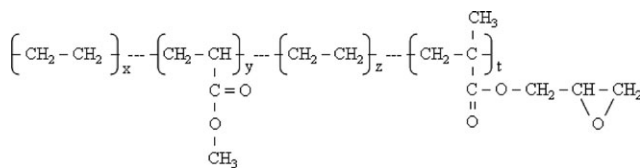Biodegradability of a polymer sample can be accessed by its consequences on other properties of the material that can be evaluated by performing visual observations, weight loss measurements, changes in mechanical properties, and molar mass after biodegradation, or directly evaluated by measuring CO_2 production or O_2 consumption during biotic among others [38]. Among these techniques, one of the most used and most accurate in determining the actual conversion of the substrate into end products is the one that measures the CO_2 evolution over the course of the biodegradation test. The CO_2 production can be monitored automatically by infrared and paramagnetic detectors, and also by manual titration, which is the most conventional method used [38]. The Sturm test is extensively used as a manual method where the CO_2 is trapped in a barium hydroxide solution, which is then titrated with hydrochloric acid [39]. Although this method is largely widespread and generally accepted, it requires a considerable amount of equipment including three scrubbing flasks and an air compressor. Another possible way to measure manually the CO_2 produced during the biodegradation of polymers is by the use of a Bartha respirometer, which was originally developed for determining the biodegradation of pollutants in soil [40–43]. In this work, it was used to evaluate the biodegradation of the materials studied. To our knowledge, it was seldom used for polymers and it consists of a much simpler device than the Sturm test [44, 45].

In view of the above, the purpose of this work was to evaluate the effect of prior photodegradation on the biodegradation of PP/PHB blends as such a study has never been conducted with blends involving poly(hydroxyalkanoates). The effect of biodegradation on the blends of different concentrations was evaluated by weight loss tests and the effect of prior photodegradation on the biodegradation of the different materials was evaluated measuring the carbon dioxide formed as the product of biodegradation process by Bartha respirometric tests. All samples were exposed to UV light for 4 weeks and further evaluated in terms of crystallinity, melting temperature, chemical structure, and biodegradation. In order to understand the effect of prior photodegradation on biodegradation the molecular weight and chemical structure of both blend components individually and within the blend (the 80/20 blend was considered as a reference) after photodegradation and/or biodegradation was studied.

EXPERIMENTAL

Materials

Poly(propylene-*co*-ethylene) (PP) (RP200L) containing 2.5 wt% of ethylene from Suzano Petroquímica (Brazil) (melt flow index (MFI) of 6 g/10 min) and PHB (B1000) from Biocycle (Brazil) (MFI of 13 g/10 min) were used in this work as the main constituents of the PP/PHB blend. The PP used in this work did not contain any pro-oxidant or other additives. The PHB used was produced from microbial fermentation using saccharose from sugarcane as the carbon source to the bacteria. The biopolymer

$$\left[CH_2 - CH_2 \right]_x \cdots \left[\begin{array}{c} CH_2 - CH \\ | \\ C=O \\ | \\ O \\ | \\ CH_3 \end{array} \right]_y \cdots \left[CH_2 - CH_2 \right]_z \cdots \left[\begin{array}{c} CH_3 \\ | \\ CH_2 - C \\ | \\ C-O-CH_2-CH-CH_2 \\ \| \quad\quad \backslash O / \\ O \end{array} \right]_t$$

SCHEME 1.   Chemical structure of the compatibilizer used.

was provided as an off-white powder and used without further purification. Poly(ethylene-co-methyl acrylate-co-glycidyl methacrylate) [P(E-MA-GMA)] (see structure in Scheme 1) containing 24 wt% of MA and 8 wt% of GMA from Arkema (France) (Lotader® AX8900) (MFI of 6 g/10 min) was used as a compatibilizer. This compatibilizer was shown to be efficient for PP/PHB blend in a previous study from the authors [9].

Preparation of Blends

PHB, in powder form, was first pelletized. Then, PP/PHB blends were obtained in four different weight compositions (90/10, 80/20, 70/30, and 60/40). A compatibilized blend with 80/20/10 [PP/PHB/P(E-MA-GMA)] composition was also prepared. All blends were prepared in two steps. In a first step, P(E-MA-GMA) was mixed with PP and the resultant blend was further mixed with PHB. In the case of the noncompatibilized blends, PP was first processed to have undergone the same thermomechanical history as in the compatibilized blends and further blended to PHB. The pelletization and preparation of all blends was performed using a twin-screw extruder Haake Rheomix PTW 16 operating at 160°C. The preparation of the blends was performed at a screw speed of 50 rpm and feeding speed of 10 rpm, while the pelletization of PHB was undertaken at faster speeds (110 and 50 rpm, respectively), due to the high MFI presented by this material. The temperature used was chosen as the minimum one at which PHB could be completely molten in an attempt to minimize its well-known thermal degradation [46–48]. The materials were further injection-molded in a Demag Ergotech machine at 170°C and at a screw speed of 160 rpm.

Photodegradation

The molded samples were exposed to artificial UV radiation a few days after injection to take into account the change of morphology of the sample after processing as it is well known that the crystallinity and morphological structure of PHB evolves at room temperature after processing [4–6]. For UV radiation exposure, an accelerated weathering chamber QUV from Q-Panel (Cleveland, OH) containing 8 UV-A fluorescent lamps was used. The lamps of the weathering chamber have a maximum irradiance of 0.89 W/m^2 at 340 nm. This wavelength presents a good correlation with the sunlight spectrum. The weather-ing cycles were defined as follows: 8 h under UV light at 60°C and 4 h in the dark under condensed water at 50°C. The exposure time used was 4 weeks and the dimensions of the sample were $70 \times 13 \times 0.8$ mm^3 (length × width × thickness).

Biodegradation

Weight Loss Tests. Before UV exposure, an initial study of the composition influence on the biodegradability of the samples was performed by means of the weight loss test. Individual PP, PHB, or blends of different concentrations were exposed to simulated compost containing equal parts (by weight) of soil, sand, and manure as suggested by the ASTM D5988 standard [49]. The compost used was analyzed in terms of its macronutrients and some other parameters, results are shown in Table 1. Specimens were cut into dimensions of $10 \times 13 \times 0.8$ mm^3, buried in trays, and incubated in the dark inside an oven maintained at 30°C. Distilled and deionized water was added to the compost every week to bring the moisture content to 30%. Periodically, the samples were taken from the trays, carefully washed with water, dried in a vacuum oven at 55°C for approximately 20 h, and weighed on a Shimadzu analytical balance model AUW220D. Approximately six measurements were performed for each type of sample. Weight loss was determined by the following equation:

$$\text{Weight loss}(\%) = \left(\frac{W_0 - W_t}{W_0} \right) \times 100 \qquad (1)$$

where W_0 and W_t are the weight of the samples before burial and after burial for a given time, respectively.

Bartha Respirometry. The samples exposed to UV radiation could not be evaluated by the weight loss test. After photodegradation, the samples containing a high content of PP were very brittle and easily broken by handling, thus their biodegradability evaluation by the weight loss test would lead to nonprecise results. Therefore, the effect of photodegradation on biodegradation was assessed

TABLE 1.   Analysis of the soil used in the weight loss and respirometric tests.

Parameters	Unit	Value
pH	–	5.7
Organic matter	g/dm^3	74
C	%	10.9
N	%	0.53
S	%	0.08
P	mg/dm^3	296
K	Mmolc/dm^3	14.1
Ca	Mmolc/dm^3	112
Mg	Mmolc/dm^3	62
H + Al (total acidity)	Mmolc/dm^3	31
CEC	Mmolc/dm^3	219.1

Legend:

A – Cannula cover

B – Cannula

C – Rubber cork

D – Side arm

E – KOH solution

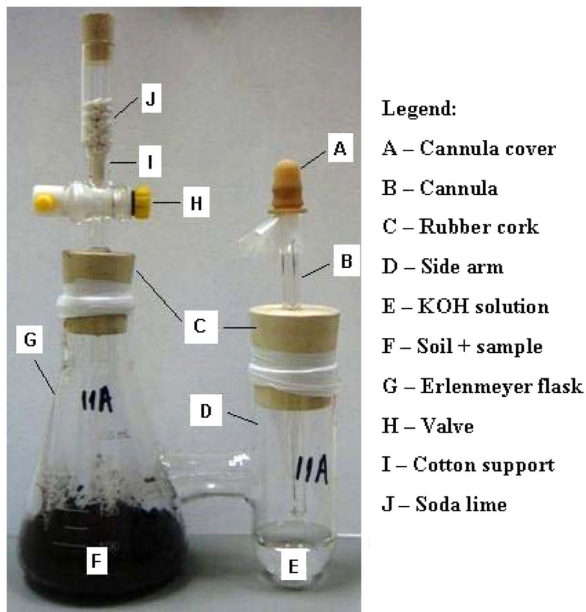F – Soil + sample

G – Erlenmeyer flask

H – Valve

I – Cotton support

J – Soda lime
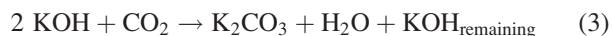
FIG. 1. Bartha respirometer. [Color figure can be viewed in the online issue, which is available at wileyonlinelibrary.com.]

evaluating the CO_2 produced during the biodegradation of polymers using a Bartha respirometer [40–42] as illustrated in Fig. 1 following the Brazilian standard ABNT NBR 14823:1999.

In a typical test, the samples are placed in an Erlenmeyer flask (G) together with the soil mixture described in the weight loss test containing a water content of 60% of its field capacity, as recommended by the standard. Air, free of CO_2 which is absorbed by Soda lime (J), is injected into the upper side of the Erlenmeyer flask through a hose connected to an oxygen cylinder. Aerobic biodegradation takes place in the Erlenmeyer flask producing CO_2 gas as shown in chemical Eq. 1. The CO_2 is trapped in the side arm of the respirometer reacting by a KOH 0.4 N solution (chemical Eq. 3). This solution is taken from the respirometer weekly and titrated with a HCl 0.1 N solution (chemical Eq. 4). A fresh KOH solution is added to the respirometer after the whole system is aerated for 5 min. Then the whole set up is re-incubated inside an oven maintained at 30°C until next measurement.

$$C_{polymer} + O_2 \rightarrow CO_2 + H_2O + C_{residue} \qquad (2)$$

$$2\ KOH + CO_2 \rightarrow K_2CO_3 + H_2O + KOH_{remaining} \qquad (3)$$

$$KOH_{remaining} + HCl \rightarrow KCl + H_2O \qquad (4)$$

The amount of CO_2 produced in each respirometer can be calculated using Eq. 5:

$$mgCO_2 = (A - B) \times 2.2 \times f_{HCl} \qquad (5)$$

where A is the HCl volume used to titrate the blank sample (fresh KOH), B is the HCl volume used to titrate the

KOH solution taken from the respirometer, 2.2 is the constant that relates ml of HCl with mg of CO_2, and f_{HCl} is the HCl solution factor.

In the present work, for each sample, the system was assembled in triplicate as recommended by the standard. Samples cut with the dimensions $40 \times 13 \times 0.8\ mm^3$ were placed in the Erlenmeyers. A set of three control respirometers containing only the soil mixture was also tested.

The results were expressed in terms of biodegradation degree, which was calculated by dividing the amount of CO_2 obtained by the theoretical amount of CO_2 that should be produced in each respirometer. The theoretical CO_2 was obtained by the following equation:

$$Theoretical\ CO_2 = \frac{44 \times C_i \times m}{12} \qquad (6)$$

where C_i and m are the carbon content and mass of each sample, respectively. The carbon content was estimated theoretically for each polymer and blend considering their compositions. As each respirometer contained was also taken into account.

The amount of CO_2 produced in the respirometers containing the polymer and the soil was subtracted from the result obtained in the control respirometer (containing just the soil) in order to yield the amount of CO_2 and, therefore, the biodegradation degree related only to the polymer sample. The soil also produces CO_2 due to its organic matter (Table 1).

It was checked that the system was properly sealed using the bubble test and titrating a KOH solution kept inside an empty (without soil or sample) respirometer for a week. The result yielded the same value as the titration of a fresh KOH sample indicating that the KOH inside the respirometer was not absorbing CO_2 from outside.

Characterization Techniques

The morphological observations of the surface were performed on the individual polymers or blends before and after photodegradation and/or biodegradation. In order to understand the influence of prior photodegradation on the biodegradation of the different samples studied (individual polymers and blends), Fourier transform infrared spectroscopy (FTIR) and size exclusion chromatography (SEC) analyses of PP and PHB before and after degradation (photodegradation and/or biodegradation) were carried out. SEC analyses of PP and PHB phases within the 80/20 noncompatibilized blends were also performed. FTIR of the blend samples could not be performed as the carbonyl band of photo-oxidized PP would be overlapped with the one of PHB. The analysis (SEC) of the samples after degradation was performed using samples from an upper layer (0.1 mm from the exposed surface). To evaluate the molar mass by SEC of PP or PHB phases within the blend, entire samples (before or after degradation),

that is, samples were submitted to selective extraction. PP was separated by successive washing of the blend in toluene (at a temperature of about 110°C) followed by filtration and precipitation by addition of acetone to the solution. Toluene was chosen because previous tests showed that this solvent would dissolve PP without attacking PHB. The separation of PHB was performed washing the blend in chloroform (at a temperature of about 55°C) followed by filtration and precipitation in solution adding methanol to the system.

Scanning Electron Microscopy. The morphology of the blends as well as the surface of the different materials after photodegradation and/or biodegradation were observed using a Scanning Electron Microscope Philips XL 30 with a voltage of 20 kV after the materials were coated by gold sputtering. To study the morphology of the blends prior to any degradation, the samples were crio-fractured after cooling in liquid nitrogen before the sputtering.

Size Exclusion Chromatography. Size-exclusion chromatography (SEC) analyses of PHB samples were conducted using a Waters equipment with three columns phenomenex 5 μ Phenogel linear (7.8 $\times$ 300 mm^2) and a precolumn connected in series at a temperature of 30°C, with a refractive index detector Waters 2414 at a temperature of 40°C. PHB was dissolved in HPLC chloroform and the filtered solution injected into the equipment containing as the mobile phase chloroform at a flow rate of 1 ml/min. The columns were calibrated with narrow molecular weight polystyrenes samples. The SEC analyses of PP were carried out using a chromatograph Polymer PL 220 model equipped with a refractive index and a viscosimetric detector. The equipment contained four columns Toso-Hass (HT3, HT4, HT5, and HT6), a precolumn (500 Å) and was operated at a temperature of 150°C. PP was dissolved in HPLC grade 1,2,4-trichlorobenzene together with 0.1 g/l of the thermostabilizer 2,6-di(*tert*-butyl)-4-methylphenol and the filtered solution was injected into the equipment which used a solvent flow rate of 1 ml/min. The equipment was calibrated with a series of monodisperse polystyrene standards. The calibration curve was validated using a polydispersed polyethylene standard sample NBS 1475 following the procedures of Hoeve et al. [50].

Fourier Transform Infrared Spectroscopy. FTIR was carried out using a Nicolet Magna 560 spectrophotometer. The samples analyzed were thin films melt pressed from sections of the materials containing their initial thickness (0.8 mm) since it would be very difficult to obtain continuous films only from the particles contained in the degraded surface of the samples. The analysis was made with thin films by transmission and 64 scans were accumulated at a resolution of 4 cm^{-1}.

UV/Visible Spectroscopy. UV/Visible spectroscopy (UV/VIS) in the transmittance mode was performed in a Shimadzu Multispec 1501 spectrophotometer using solid samples containing their initial thickness (0.80 mm).

RESULTS AND DISCUSSION

Effect of Blend Composition and Compatibilization

The morphological observations of cryogenic fractures of the blends revealed that all the blends studied (with concentrations ranging from 90/10 to 60/40) with and without compatibilizer presented a morphology of dispersed PHB droplets within a PP matrix (data not shown here). Also, as the concentration of PHB increased, the diameter of the dispersed phase increased due to coalescence of dispersed phase during processing [51, 52] and when P(E-MA-GMA) was added to the blend the size of the dispersed phase decreased and a better adhesion between PHB and PP phase was observed evidencing the compatibilization effect of P(E-MA-GMA) due to a chemical reaction between the epoxy group of P(E-MA-GMA) and the carboxylic acid group from the chain end of PHB [9].

Figure 2 presents the weight loss for the different blends (not exposed to UV light) studied here, as a function of time. Figure 2b presents the weight loss of the blends after 306 days of biodegradation and an "extrapolated" weight
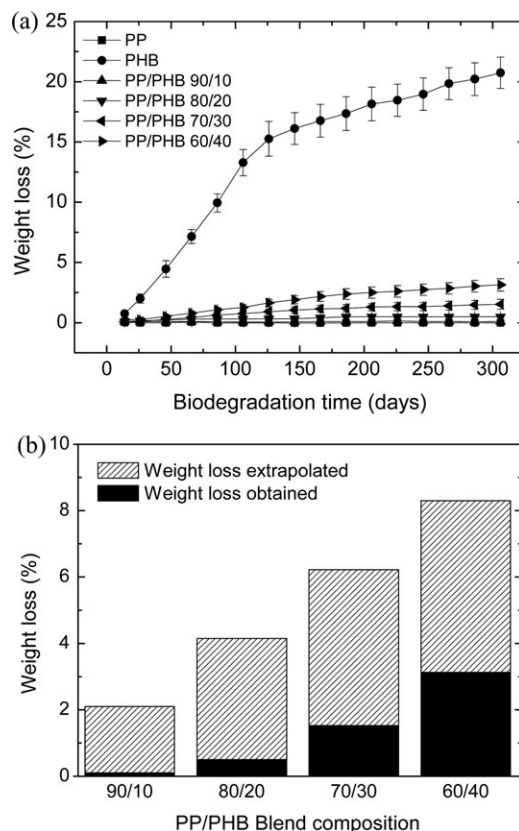

FIG. 2. Weight loss of the materials without exposure to UV radiation: (a) values obtained for the blends and pristine polymers and (b) values obtained and extrapolated for the blends.
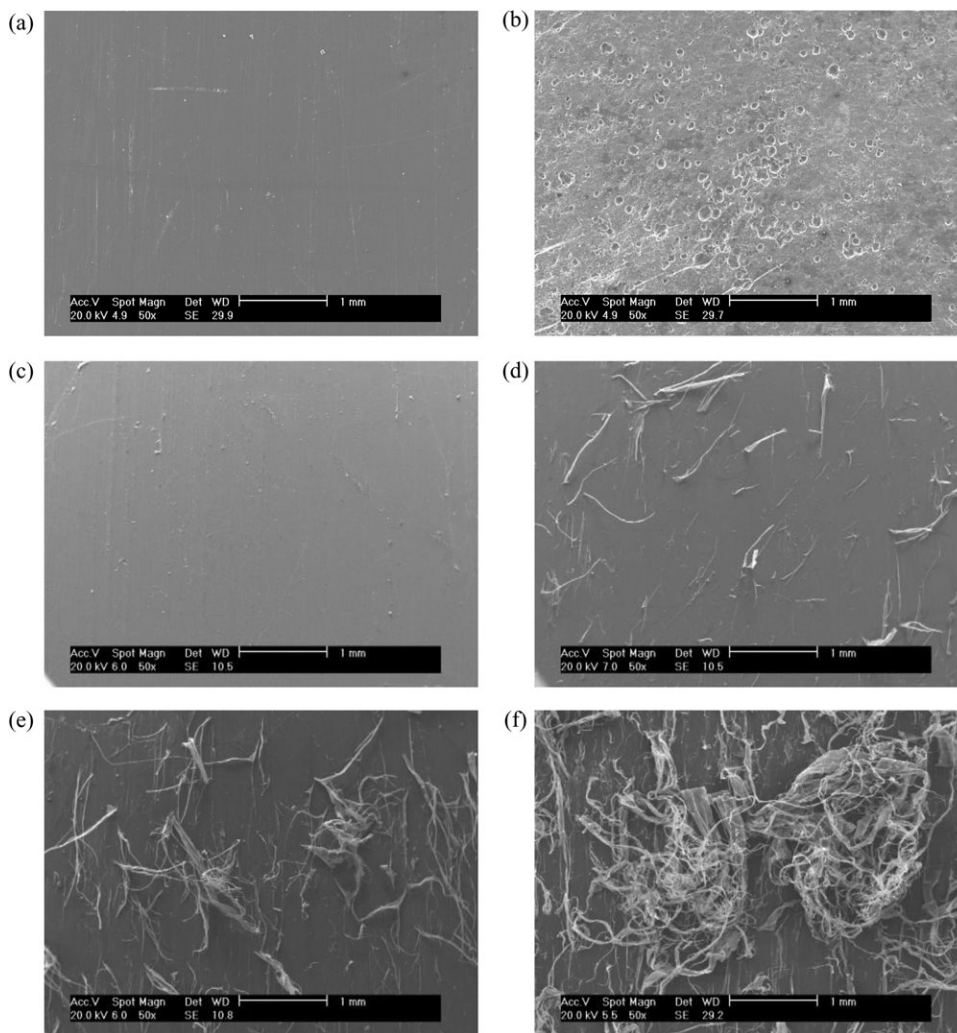
FIG. 3.   SEM of the samples surface after 306 days of the weight loss test: (a) PP, (b) PHB, (c)PP/PHB 90/10, (d) PP/PHB 80/20, (e) PP/PHB 70/30, and (f) PP/PHB 60/40.

loss that would have been obtained if the PHB within the blends had biodegraded at the same rate as the individual PHB. It can be seen that PHB presents high values of weight loss, whereas PP does not show any biodegradation. It can be seen that the weight loss reaches higher values as the concentration of PHB increases within the blends. Similar behavior has already been observed in the literature [53]. It can also be seen that the weight loss experimentally obtained is much lower than the extrapolated one indicating that the biodegradation of PHB was hindered within the blends. The data also show that the ratio weight loss experimentally evaluated/extrapolated weight loss increased with increasing concentration of dispersed phase. These results can be explained in light of the morphology of the blends. Within the blends, the only phase that is biodegradable is PHB, which forms a noncontinuous phase of dispersed droplets within a matrix of PP. When the micro-organisms are in contact with the blends, they do not encounter a continuous phase of biodegradable material, but particles separated from each other, and as the concentration of the dispersed phase increases, the size of the dispersed phase

increases explaining the increase in the ratio of weight loss shown in Fig. 2. Moreover, blends obtained by injection molding [54] present a profile of morphology with a skin of matrix (in the case of the blends studied here PP) phase at their surface also contributing for the slower biodegradation of the blend when compared to the one of individual PHB. The results obtained here are in good agreement with the experimental results of several researchers [33–36] and with the theories of percolation developed by the research group of Wool [31, 32, 34]. This theory suggests the existence of a percolation threshold, which is the minimal amount required of the biodegradable material to achieve connectivity between its domains and therefore to allow accessibility of the micro-organisms to its chains. The results of morphology and biodegradation presented indicate that for the system and processing conditions used in the present work the maximum content used of 40% PHB is still below the percolation threshold.

Figure 3 shows the superficial morphology of the different samples after 306 days of biodegradation. It can be seen that the PP/PHB blends with higher concentration of

PHB present a fibrous structure at their surface. The presence of this structure, which could be seen visually, seemed to increase with increasing time of biodegradation. As PP is the continuous phase in the blends, these particles are likely to consist of PP phase, which was not consumed during the biodegradative process and was released from the blends as PHB was decomposed.

Figure 4 shows the biodegradation degree for 80/20 noncompatibilized and compatibilized blends. The results seem to indicate that the compatibilized blend suffers less biodegradation. These results could be due to a smaller size of the PHB nodules or to the dilution effect resultant from the addition of 10 wt% of the compatibilizer P(E-MA-GMA) which is not biodegradable. Very few studies of the effect of compatibilization on biodegradation have been conducted in the literature but a slower biodegradation for compatibilized blends has already been observed in the case of polycarbonate/polylactic acid blends [55]. An observation of the surface of the compatibilized blend after biodegradation did not show the particles that were observed in Fig. 3 for the non compatibilized blend (see Fig. 3d) which is in good agreement with the smaller biodegradation observed.

Effect of Prior Photodegradation

The effect of prior photodegradation on biodegradation was studied using samples that had been exposed to UV light for 4 weeks in the conditions reported in experimental methods. In the remaining of the text, the materials which were not exposed to either photodegradation nor biodegradation will be referred to as non-degraded materials, the ones that were exposed only to UV light will be named photodegraded materials, the ones that were exposed only to biodegradation will be referred to as biodegraded materials and the ones that were exposed to both photo and bio degradation will be named photobiodegraded materials.

Production of CO_2 and Weight Loss During Biodegradation. Figure 5 shows the biodegradation degrees for non-degraded and previously photodegraded samples. The values showed represent an average of three measurements for each sample. Here the data for isolated PP and PHB as well as 80/20 compatibilized or not blends are presented. The data for the other blends are not shown as they presented the same trend. It can be seen from Fig. 5 that a prior exposure to UV light hindered the biodegradation of PHB (such behavior was already presented and discussed in more details in a previous study from the authors [17]) whereas it enhanced the one of PP and the blends. Enhancements of biodegradation after UV exposure have already been reported in the literature [10–12, 18, 23].

The biodegradation values of PHB and PP/PHB 80/20 blend (12 and 3%, respectively, before exposure to UV light) obtained for the time studied in this work (56 days) are lower than other values reported in the literature (24%
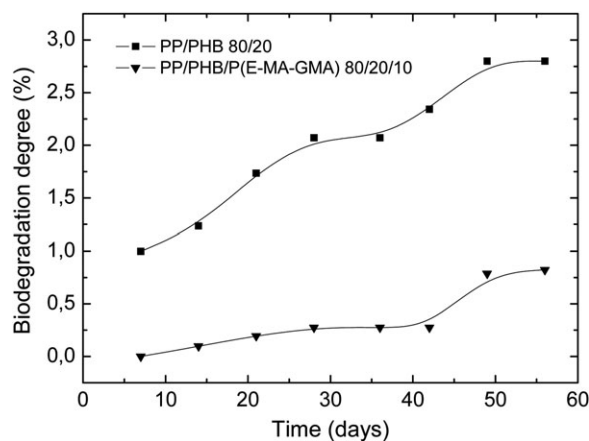

FIG. 4. Biodegradation degree of PP/PHB 80/20 and PP/PHB/P(E-MA-GMA) 80/20/10 blends before exposure to UV light. These results correspond to samples with 0.8 mm thickness, which leads to the low biodegradation degree observed.

for poly L lactic acid (PLLA) and 10% for ethylene vinyl alcohol copolymer/PLLA 60/40 blend after 23 days [56], 60% for cellulose and 10% for LDPE/cellulose 50/50 blend after 30 days [24], 25% for PLLA after 23 days [57], and 20% for PBS after 35 days [58]). This can be mainly attributed to the difference in the specimen thickness used in such studies. While in the present study a thickness of 0.8 mm was used, in the other studies mentioned a smaller thickness was employed (0.1 mm [58], 0.2 mm [56, 57], and 0.5 mm [24]). Since biodegradation is a superficial process, samples with greater thickness are expected to biodegrade at a lower rate. Furthermore, thicker samples usually do not decompose completely upon the biodegradation time studied, allowing them to be analyzed by other physical/chemical methods after biodegradation, which complement the results obtained.

Sample Morphology and Physical Aspect of the Samples. Figures 6 and 7 show the morphologies of the surface of PP, PHB, and PP/PHB 80/20 blends compatibilized or not prior and after photo/or biodegradation in the respirometer. It can be seen that surface erosion occurred for PHB after the biodegradation test whereas no change of surface could be observed for PP. These results are expected due to the chemical nature of these polymers. UV exposure resulted in surface cracks for PP and its blends with PHB. This crack formation is related to chemi-crystallization process that causes densification of surface layers and ultimately leads to spontaneous cracking [59] and has been observed in several studies [60]. The surface of PHB seems to have not been affected by UV light and the occurrence of cracks was less severe for the blends than for the pristine PP, most likely due to a better photostability of PHB than PP [17]. Also, when PHB is added to PP, the samples become darker and the penetration of UV light is reduced as PHB content raises [17]. The cracks formed during UV radiation on the
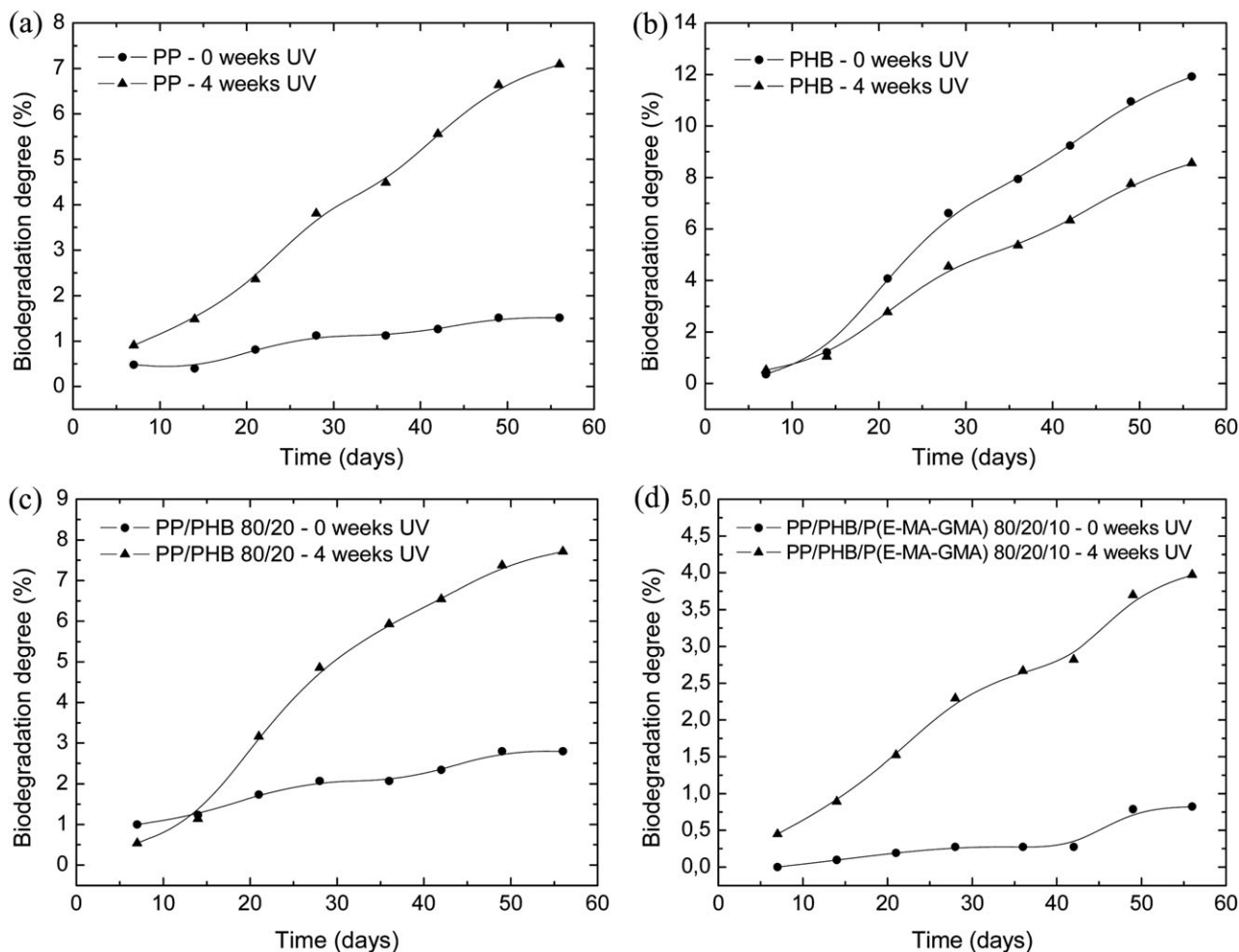
FIG. 5. Biodegradation degree of: (a) PP, (b) PHB, (c) PP/PHB, and (d) PP/PHB/P(E-MAGMA) 80/20/10 exposed or not to UV radiation for 4 weeks. These results correspond to samples with 0.8 mm thickness, which leads to the low biodegradation degree observed.

surface of the samples may have facilitated the access of oxygen and enzymes to deeper layers of the samples, increasing the biodegradation reactions for both PP and the blends.

The morphologies of the materials after photo and biodegradation do not present drastic changes when compared to the ones of the samples that was only photodegraded. However, no fibrous structure could be observed on the surface of blend samples which were both photo and biodegradaded as it was observed on the surface of the sample that only had been subjected to biodegradation (Fig. 3). This possibly occurs because the PP remaining in the samples with its molecular weight reduced by the action of UV radiation (as will be shown further) did not present enough integrity for the formation of continuous particles.

Figure 8 presents the physical aspects of PP, PHB, and PP/PHB 80/20 and 60/40 blends prior any degradation and after photodegradation and/or biodegradation. It can be seen that UV exposure resulted in a change of color for all the samples: PHB and the blends whitened prob-

ably due to a change of surface roughness and crystallinity [17] whereas PP became yellower due to the formation of chromophores that can absorb visible light. It can also be seen that biodegradation after UV exposure resulted in much more changes of the sample surfaces than biodegradation alone: PHB had part of its white surface consumed and the blends presented the formation of color spots that can be attributed to fungus attack [17]. Similar observations were made by Okamoto et al. [61] who studied the biodegradation of PBS clay containing nanocomposites. In the present work, after biodegradation without prior photodegradation, these color spots were only observed on the surface of the blends with greater PHB content (30 and 40%), while after UV exposure followed by biodegradation this behavior was not only more severe in these materials as it could already be observed for the blends with minor PHB content. Also PP and the blends present dark spots at their surface which are soil particles remaining in the samples that could not be washed out as they were probably retained in the cracks formed during photodegradation. These observations indicate that prior
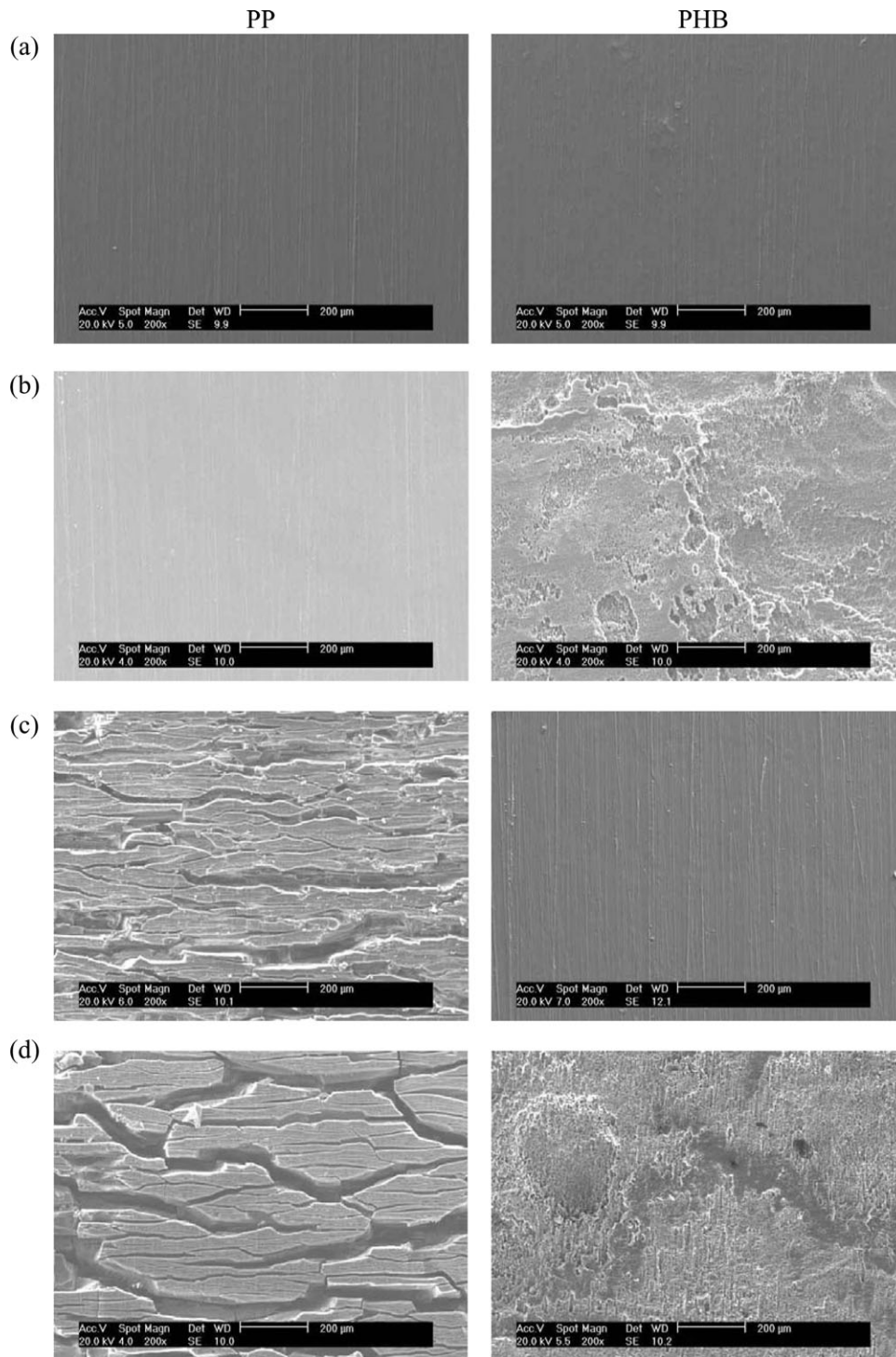
PP   PHB

FIG. 6.   SEM micrographs of the surface of PP (first column) and PHB (second column): (a) without degradation, (b) after the respirometry test for 56 days, (c) after UV exposure for 4 weeks, and (d) after UV exposure for 4 weeks and the respirometry test for 56 days.

photodegradation was indeed effective in helping the biodegradation of the blends, or at least was able to contribute to a better adhesion of micro-organisms to the polymer surfaces.FTIR – SEC

The results shown in Figs. 5–8 indicate that prior exposure to UV light affected the biodegradation of both

PHB and PP. The reasons for the slower biodegradation of PHB after UV exposure for the time duration studied are discussed in details somewhere else [17]. The increase of biodegradability of PP is probably related to the formation of chains with lower molecular weight containing hydrophilic groups during UV exposure, which was

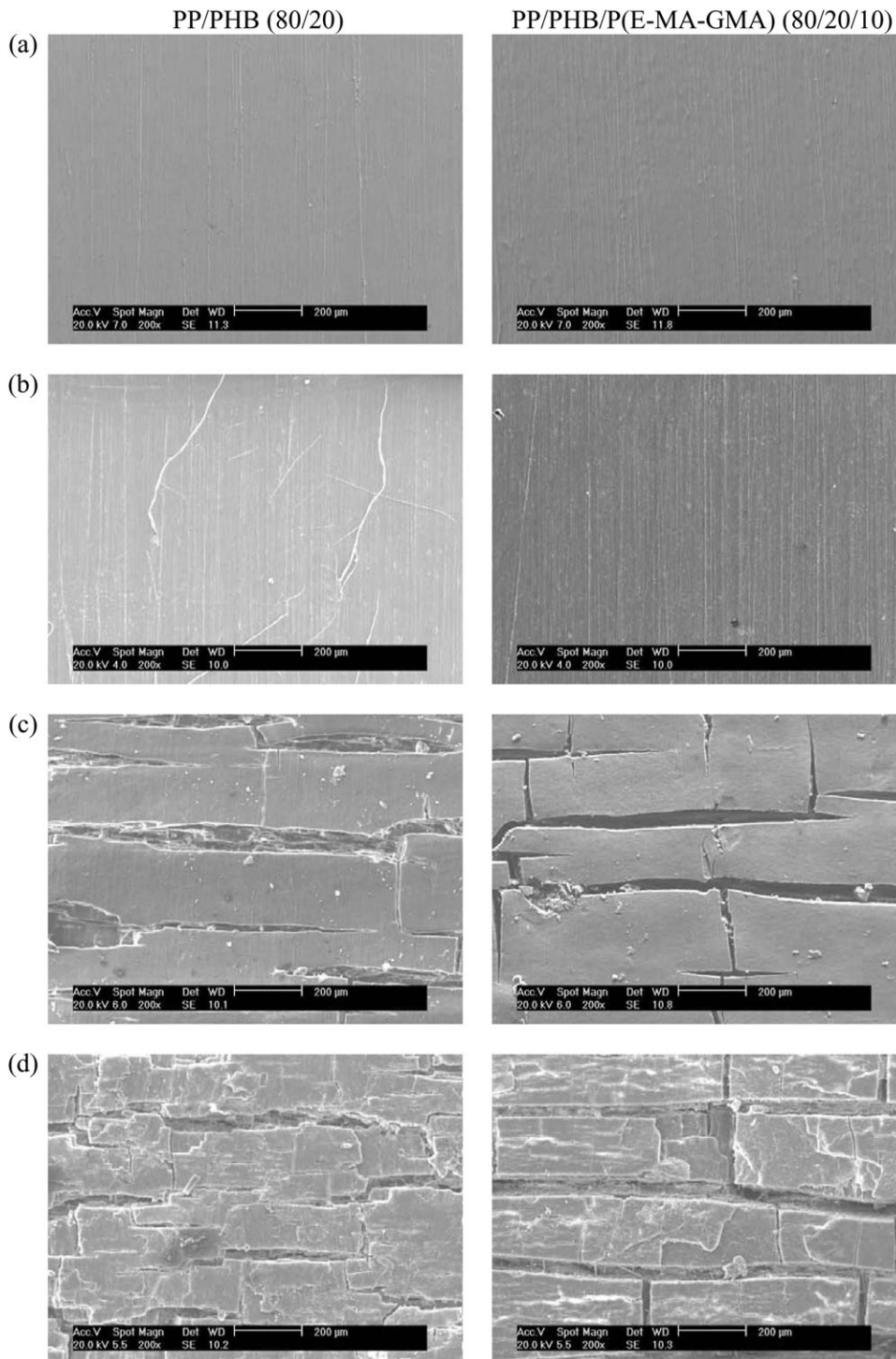PP/PHB (80/20) PP/PHB/P(E-MA-GMA) (80/20/10)

(a)

(b)

(c)

(d)

FIG. 7. SEM micrographs of the surface of PP/PHB 80/20 (first column) and PP/PHB/P(E-MAGMA) 80/20/10 (second column) blends: (a) without degradation, (b) after the respirometry test for 56 days, (c) after UV exposure for 4 weeks, and (d) after UV exposure for 4 weeks and the respirometry test for 56 days.

monitored in this work by FTIR and SEC analysis. PP was shown to dissolve readily in xylene after photodegradation indicating that photodegradation did not result in crosslinking in this material despite the 2 wt% of PE within its chain.

Prior UV exposure also resulted in an accelerated biodegradation of the blends. Photodegradation of blends is a very complex subject that is not fully understood yet. The photodegradation of a blend may not only be considered as merely an additive effect of the photodegradation of
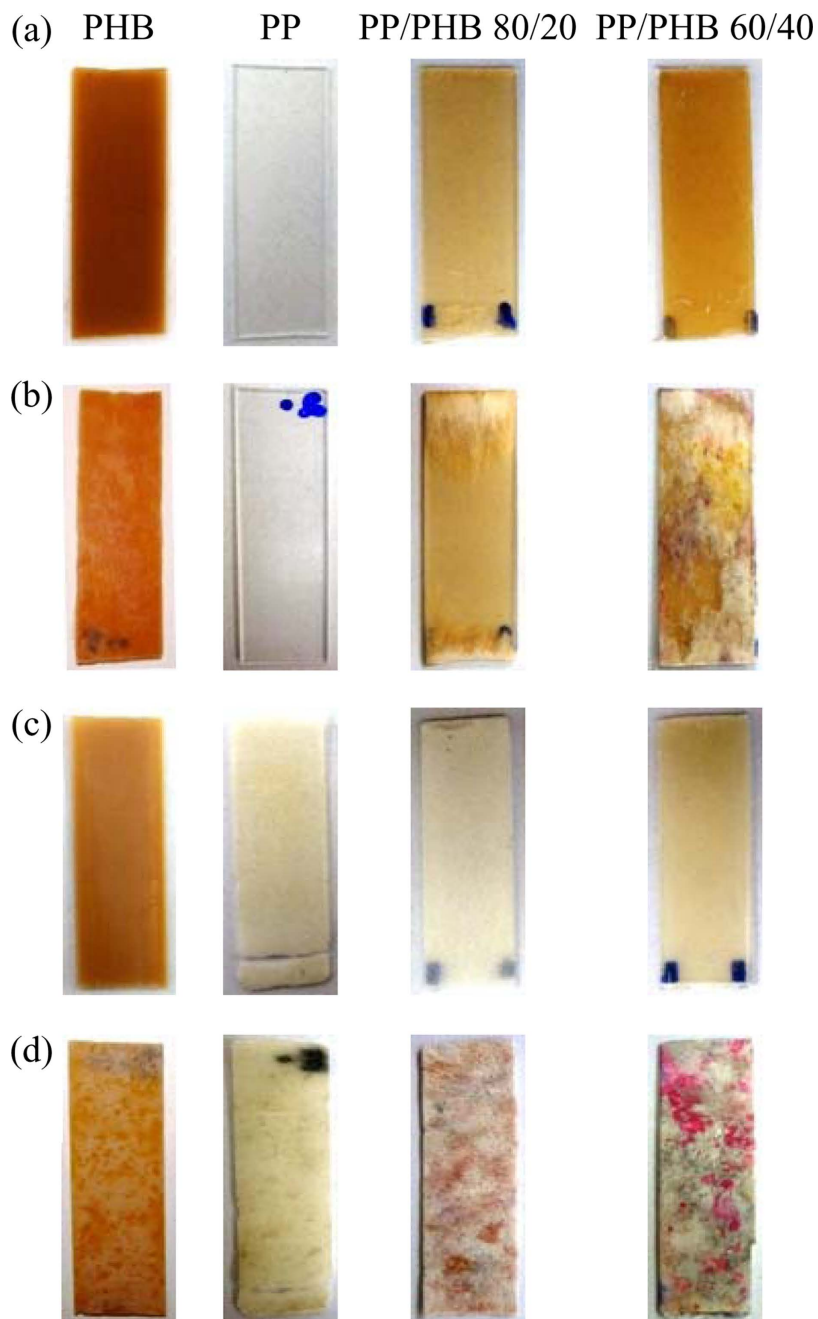
FIG. 8. Photographs of PHB (first column), PP (second column) blends, PP/PHB 80/20 (third column), and PP/PHB 60/40 (fourth column): (a) without degradation, (b) after the respirometry test for 56 days, (c) after UV exposure for 4 weeks, and (d) after UV exposure for 4 weeks and the respirometry test for 56 days. [Color figure can be viewed in the online issue, which is available at wileyonlinelibrary.com.]

each of its components. Migration of free radicals and small molecules originated from the photodegradation process of one of the phases, of additives, as well as energy transfer may occur from one polymer to another [62]. Thus, the effects can be diverse: it may happen that a component of the blend has its photodegradation suppressed or enhanced when compared with the original polymer. Understanding the mechanism of photodegradation of the PP/PHB blend is out of the scope of the present

artcle. Here, photodegradation was evaluated as a tool to accelerate the biodegradation of PP/PHB blends. The reasons for this possible acceleration will be discussed below in light of the chemical changes undergone by PP and the decrease of molecular weight of either polymer within the blends during photodegradation. For that, the composition 80/20 was chosen as a representative PP/PHB blend.

Table 2 presents the carbonyl and hydroperoxide index for PP prior to photo and biodegradation and after UV

TABLE 2. Carbonyl and hydroperoxide indexes of PP before and after UV exposure for 4 weeks and/or biodegradation in the respirometer for 56 days.

Degradation type	Carbonyl index	Hydroperoxide index
–	0.33	0.28
Biod	0.25	0.28
UV	7.80	5.50
UV/Biod	3.55	2.20

exposure and/or biodegradation. These indexes were calculated as follows.

$$\text{Carbonyl index} = \text{Abs } 1712 \text{ cm}^{-1}/\text{Abs } 2720 \text{ cm}^{-1} \quad (6)$$

$$\text{Hydroxyl index} = \text{Abs } 3450 \text{ cm}^{-1}/\text{Abs } 2720 \text{ cm}^{-1} \quad (7)$$

It can be seen from Table 2 that some of the carbonyl and hydroperoxides generated by photodegradation were consumed during the biodegradation of PP. These results are in good agreement with results previously reported in the literature, which indicated the reduction of the carbonyl band after the biodegradation of LDPE [14, 16, 17] PP [14] and PP-g-MAH/coconut fiber composites [23]. This could be due to the release of short-chain carboxylic acids in the form of degradation products during the biotic stage [10].

The molecular weights of the samples of pristine PP and PHB as well as their phases within the blends prior and after photodegradation and or biodegradation are presented in Tables 3 and 4. It can be seen from these tables that the molecular weights of either PP or PHB (pristine or within the blend) decrease after UV exposure. However, the molecular weight of PHB decreases in a lower extent due to the better photostability of this polymer [17]. Table 5 presents the distributions of molecular weight of PP within and not within the blend before and after photodegradation. It can be seen that before UV exposure, most of the PP chains had a molecular weight larger than 100,000 whereas after photodegradation most of the chains had a molecular weight smaller than 10,000. Table 3 also shows that there was a small decrease in the molar mass of PP after biodegradation without prior expo-

TABLE 3. Molar mass of pristine PP and PP within PP/PHB 80/20 blend before and after UV exposure for 4 weeks followed or not by biodegradation in the respirometer for 56 days.

Material	Degradation type	$\overline{M}_w$	$\overline{M}_n$	$\overline{M}_w/\overline{M}_n$
Pristine PP	–	234,000	64,700	3.61
	UV	6600	1800	3.64
	Biod.	208,200	58,700	3.54
	UV/Biod.	8200	3600	2.27
PP (blend 80/20)	–	269,600	67,800	3.98
	UV	12,100	4500	2.69

TABLE 4. Molar mass of pristine PHB and PHB within PP/PHB 80/20 blend before and after UV exposure for 4 weeks followed or not by biodegradation in the respirometer for 56 days.

Material	Degradation type	$\overline{M}_w$	$\overline{M}_n$	$\overline{M}_w/\overline{M}_n$
Pristine PHB	–	136,700	62,000	2.20
	UV	55,800	21,300	2.62
	Biod.	131,400	59,400	2.21
	UV/Biod.	45,800	15,200	3.02
PHB (blend 80/20)	–	143,600	49,400	2.91
	UV	38,000	9300	4.09

sure to UV radiation. This behavior has also been reported for PP [10] and polyethylene [10, 24] and should be related to either breakage of the chains of low molar mass of PP by micro-organisms (Table 5 shows a small fraction of molecules in this range) or to differences of sampling. Biodegradation preceded by photodegradation resulted in an increase of PP molecular weight. This behavior could also occur for some difference in sampling (as photodegradation of PP is a heterogeneous process [63], or be due to consumption of part of the chains of low molecular weight generated by photodegradation). The results presented in Table 4 show that the decrease of molecular weight of PHB after biodegradation is relatively small considering that this polymer is biodegradable. However, one should remember that the fraction of the sample evaluated is the one that has not biodegraded yet or was partially consumed by the micro-organisms, maintaining part of its original properties. Although the drop of molar mass after biodegradation for PHB was of the same order of magnitude as the one for PP, PHB biodegraded much more as can be seen in Figs. 2 and 5. Furthermore, the PHB sample presented a great drop of its thickness after biodegradation, whereas PP did not present any visual modification. The decrease of molecular weight of PHB after biodegradation preceded by photodegradation was larger than the samples that were only exposed to the soil. This result implies that the remaining PHB sample analyzed after photo/biodegradation was in a different stage of the decomposition process.

The substantial drop of the molecular weight of polyolefins after UV exposure is a well-known phenomenon

TABLE 5. Distribution of molar masses obtained by GPC for pristine PP and PP within PP/PHB 80/20 blend before and after UV exposure for 4 weeks.

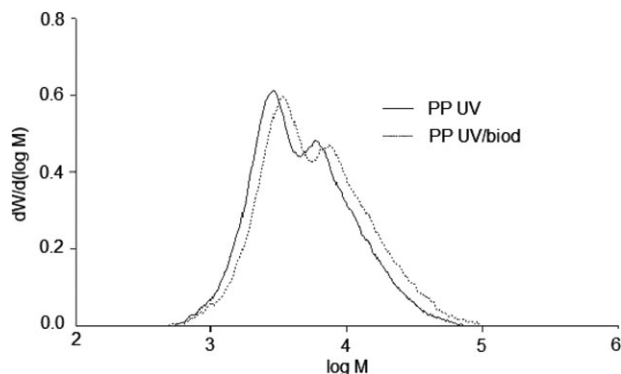| Range of molar mass	% Area			
	Pristine PP before UV	Pristine PP after UV	PP (80/20 blend) before UV	PP (80/20 blend) after UV
>1,000,000	2.3	–	3.7	–
999,999–100,000	61.0	–	61.4	0.6
99,999–10,000	34.1	29.3	32.2	33.6
<9999	2.3	70.7	2.4	65.7

FIG. 9. Molar mass distribution of PP after UV exposure for 4 weeks and after UV exposure for 4 weeks and biodegradation (respirometry test for 56 days).

[10, 12, 22, 64, 65] which together with the formation of functional groups could explain the increase of biodegradability. However, it has been reported in the literature that micro-organisms could only assimilate paraffinic chains of a molecular weight of up to 500 g/mol [66] (another study reported the rapid assimilation of oxidized fragments of PE chains with a molar mass of 40,000 g/mol [67]). The SEC histograms of the samples analyzed here indicated that the smallest molecular weight for the PP samples before and after UV exposure were 1700 g/mol and 800 g/mol, respectively. Figure 9 presents the SEC histograms of PP before and after biodegradation (preceded by photodegradation). The comparison of both histograms seems to indicate that no short chains were consumed during biodegradation. However, PP that had been previously photodegraded presented a larger CO_2 production (see Fig. 5a). Since the columns used in SEC had a lower detection limit of 500 g/mol, photodegradation could have resulted in chains with molar mass <500 g/mol which were consumed during biodegradation. This result is very important to clarify that the molecules that have not had their molecular weight drastically reduced by the action of UV radiation are not readily consumed by micro-organisms, and neither are likely to suffer any breaks during the biodegradation which would allow their quick bio assimilation.

CONCLUSIONS

The effect of blend concentration and prior photodegradation on the biodegradation of PP/PHB blends has been studied in this work. The experimental results presented, led us to conclude that the biodegradation of PHB was hindered within the blends as they presented dispersed droplet type morphology where the PHB domains did not have connectivity, turning their access by micro-organisms more difficult. Also, prior photodegradation resulted in a slower biodegradation of PHB but enhanced the biodegradation of both PP and PP/PHB blends due to the formation of carbonyl and hydroxyl group as well as

a decrease of molecular weight of PP. However, the results suggested that only the molecules that had their molecular weight drastically reduced by the action of UV radiation are readily consumed by the micro-organisms.

The addition of PHB to polyolefins may bring some biodegradability to the resultant material that can offer good mechanical properties, provided the blend morphology is properly controlled. To enhance the biodegradation of the resultant blends prior photodegradation can be used as an important tool. However, both the presence of PHB and the acceleration of biodegradation due to prior photodegradation do not turn the overall material biodegradable but more responsive to biotic reactions.

REFERENCES

1. P. Bordes, E. Pollet, and L. Avérous, *Prog. Polym. Sci.*, **34**, 125 (2009).

2. L. Yu, K. Dean, and L. Li, *Prog. Polym. Sci.*, **31**, 576 (2006).

3. C. Bastioli, *Handbook of Biodegradable Polymers*, Shawbury, UK , Rapra Technology Ltd (2005).

4. G.J.M. de Koning, A.H.C. Scheeren, P.J. Lemstra, M. Peeters, and H. Reynaers, *Polymer*, **35**, 4598 (1994).

5. G.J.M. de Koning, P.J. Lemstra, D.J.T. Hill, T.G. Carswell, and J.H. O'Donnel, *Polymer*, **33**, 3295 (1992).

6. G.J.M. de Koning and P.J. Lemstra, *Polymer*, **34**, 4089 (1993).

7. P.S. Calvão, J.M. Chenal, C. Gauthier, N.R. Demarquette, A.M. Dos Santos, and J.Y. Cavaille, *Polym. Int.*, **59**, 851 (2010).

8. C.S. Ha and W.J. Cho, *Prog. Polym. Sci.*, **27**, 759 (2002).

9. R.K. Sadi, R.S. Kurusu, G.J.M. Fechine, and N.R. Demarquette, *J. Appl. Polym. Sci.*, **123**, 3511 (2011).

10. J.K. Pandey and R.P. Singh, *Biomacromolecules*, **2**, 880 (2001).

11. P.H. Jones, D. Prasad, M. Heskins, M.H. Morgan, and J.E. Guillet, *Environ. Sci. Technol.*, **8**, 919 (1974).

12. D. Hadad, S. Geresh, and A. Sivan, *J. Appl. Microbiol.*, **98**, 1093 (2005).

13. A. Albertsson, S.O. Andersson, and S. Karlsson, *Polym. Degrad. Stab.*, **18**, 73 (1987).

14. D.S. Rosa, M.R. Calil, C.G.F. Guedes, and C.E.O. Santos, *J. Polym. Environ.*, **9**, 109 (2001).

15. V.B. Ivanov, E.Y. Khavina, S.I. Voinov, and A.A. Ol'Khov, *Int. Polym. Sci. Technol*, **36**, 19 (2009).

16. H. Tsuji, Y. Echizen, and Y. Nishimura, *J. Polym. Environ.*, **14**, 239 (2006).

17. R.K. Sadi, G.J.M. Fechine, and N.R. Demarquette, *Polym. Degrad. Stab.*, **95**, 2318 (2010).

18. H.A. Abd El-Rehim, E.A. Hegazy, A.M. Ali, and A.M. Rabie, *J. Photochem. Photobiol. A*, **163**, 547 (2004).

19. A.C. Albertsson, C. Barenstedt, and S. Karlsson, *J. Appl. Polym. Sci.*, **51**, 1097 (1994).

20. U. Ratanakammuna and A.O. Duangdao, *J. Appl. Polym. Sci.*, **100**, 2725 (2006).

21. J.M. Morancho, X. Ramis, X. Fernandez, A. Cadenato, J.M. Salla, A. Valles, L. Contat, and A. Ribes, *Polym. Degrad. Stab.*, **91**, 44 (2006).

22. H. Kaczmarek, D. Oldak, P. Malanowski, and H. Chaberska, *Polym. Degrad. Stab.*, **88**, 189 (2005).

23. J.K. Pandey, A. Ahmad, and R.P. Singh, *J. Appl. Polym. Sci.*, **90**, 1009 (2003).

24. H. Kaczmarek and D. Oldak, *Polym. Degrad. Stab.*, **91**, 2282 (2006).

25. C.F.P. Oliveira, D.J. Carastan, G.J.M. Fechine, and N.R. Demarquette, *Polym. Eng. Sci.*, **48**, 1511 (2008).

26. L.L. Fernandes, C.A. Freitas, G.J. Fechine, and N.R. Demarquette, *J. Appl. Polym. Sci.*, **120**, 770 (2011).

27. C.W. Macosko, H.K. Jeon, and T.R. Hoye, *Prog. Polym. Sci.*, **30**, 939 (2005).

28. M. Xanthos and S.S. Dagli, *Polym. Eng. Sci.*, **31**, 929 (1991).

29. D. Raghavan and A. Emekalam, *Polym. Degrad. Stab.*, **72**, 509 (2001).

30. J.B. Lee, Y.K. Lee, G.D. Choi, S.W. Na, T.S. Park, and W.N. Kim, *Polym. Degrad. Stab.*, **96**, 553 (2011).

31. J.S. Peanasky, J.M. Long, and R.P. Wool, *J. Polym. Sci. B Polym. Phys.*, **29**, 565 (1991).

32. R. Wool, D. Raghavan, G. Wagner, and S. Billieux, *J. Appl. Polym. Sci.*, **77**, 1643 (2000).

33. R. Chandra and R. Rustgi, *Polym. Degrad. Stab.*, **56**, 185 (1997).

34. S.M. Goheen and R.P. Wool, *J. Appl. Polym. Sci.*, **42**, 2691 (1991).

35. E.J. Choi and J.K. Park, *Polym. Degrad. Stab.*, **52**, 321 (1996).

36. Y. Kumagai and Y. Doi, *Polym. Degrad. Stab.*, **36**, 241 (1992).

37. A. Iwamoto and Y. Tokiwa, *J. Appl. Polym. Sci.*, **52**, 1357 (1994).

38. A.A. Shah, F. Hasan, A. Hameed, and S. Ahmed, *Biotechnol. Adv.*, **26**, 246 (2008).

39. R.N. Sturm, *J. Oil Chem. Soc.*, **50**, 159 (1973).

40. R. Bartha and D. Pramer, *Soil Sci.*, **100**, 68 (1965).

41. R.M. Atlas and R. Bartha, *Biotechnol. Bioeng.*, **14**, 297 (1972).

42. R.M. Atlas and R. Bartha, *Environ. Sci. Technol.*, **7**, 538 (1973).

43. Associação Brasileira de Normas Técnicas ABNT NBR 14823: *Resíduos em solo – Determinação da biodegradação pelo método respirométrico*, Brazilian Association of Technical norms, Sao Paulo, Brazil (1999).

44. D.S. Rosa, R.P. Filho, Q.S.H. Shui, M.R. Calil, and C.G.F. Guedes, *Eur. Polym. J.*, **39**, 233 (2003).

45. M.R. Calil, F. Gaboardi, C.G.F. Guedes, and D.S. Rosa, *Polym. Test.*, **25**, 597 (2006).

46. N. Grassie, E. Murray, and P. Holmes, *Polym. Degrad. Stab.*, **6**, 47 (1994).

47. N. Grassie, E. Murray, and P. Holmes, *Polym. Degrad. Stab.*, **6**, 95 (1984).

48. N. Grassie, E. Murray, and P. Holmes, *Polym. Degrad. Stab.*, **6**, 127 (1984).

49. ASTM D 5988-03. *Standard Test Method for Determining Aerobic Biodegradation in Soil of Plastic Materials or Residual Plastic Materials After Composting.*

50. C.A.J. Hoeve, H.L. Wagner, and P.H. Verdier, The Characterization of Linear Polyethylene SEM 1475, US Department of Commerce, National Bureau of Standard Special publication, 260 (1972).

51. A.M.C. Souza and N.R. Demarquette, *Polymer*, **43**, 1313 (2002).

52. P.S. Calvão, M. Yee, and N.R. Demarquette, *Polymer*, **46**, 2610 (2005).

53. I.M. Arcana, A. Sulaeman, K.D. Pandiangan, A. Handoko, and M. Ledyastuti, *Polym. Int.*, **55**, 435 (2006).

54. N. Walling and M.R. Kamal, *Adv. Polym. Technol.*, **15**, 269 (1996).

55. J.B. Lee, Y.K. Lee, G.D. Choi, S.W. Na, T.S. Park, and W.N. Kim, *Polym. Degrad. Stab.*, **96**, 553 (2011).

56. C.M. Lee, E.S. Kim, and J.S. Yoon, *J. Appl. Polym. Sci.*, **98**, 886 (2005).

57. C.M. Lee, H.S. Kim, and J.S. Yoon, *J. Appl. Polym. Sci.*, **95**, 1116 (2005).

58. H.S. Kim, M.O. Hwang, M.N. Kim, and J.S. Yoon, *J. Appl. Polym. Sci.*, **100**, 466 (2006).

59. M.S. Rabello and J.R. White, *Polym. Degrad. Stab.*, **56**, 55 (1997).

60. G.J.M. Fechine and N.R. Demarquette, *Polym. Eng. Sci.*, **48**, 365 (2008).

61. K. Okamoto, S.S. Ray, and M. Okamoto, *J. Polym. Sci. Part B: Polym. Phys.*, **41**, 3160 (2003).

62. W.R. Waldman and M.A. De Paoli, *Polym. Degrad. Stab.*, **93**, 273 (2008).

63. M.S. Rabello and J.R. White, *Polímeros: Ciência e Tecnologia*, **7**, 27 (1997).

64. M.S. Rabello and J.R. White, *Plast. Rubber Compos.*, **25**, 237 (1996).

65. J.M. Peña, N.S. Allen, M. Edge, C.M. Liauw, and B. Valenge, *Polym. Degrad. Stab.*, **72**, 259 (2001).

66. P. Klemchuk, *Polym. Degrad. Stab.*, **27**, 183, 1990.

67. R. Arnaud, P. Dabin, J. Lemaire, S. Al-Malaika, S. Chohan, M. Coker, G. Scott, A. Fauve, and A. Maaroufi, *Polym. Degrad. Stab.*, **46**, 211 (1994).